

We are IntechOpen, the world's leading publisher of Open Access books Built by scientists, for scientists

5,000

Open access books available

125,000

International authors and editors

140M

Downloads

Our authors are among the

154

Countries delivered to

TOP 1%

most cited scientists

12.2%

Contributors from top 500 universities



WEB OF SCIENCE™

Selection of our books indexed in the Book Citation Index
in Web of Science™ Core Collection (BKCI)

Interested in publishing with us?
Contact book.department@intechopen.com

Numbers displayed above are based on latest data collected.
For more information visit www.intechopen.com



Polyimide Used in Space Applications

Virginie Griseri

Abstract

Polyimide (PI) is an interesting material for space applications as it offers excellent thermal properties. However, due to its dielectric properties, charge storage and release can be at the origin of electrostatic discharges that are hazardous for the surrounding electrical equipment. Depending on the spacecraft orbit, it is necessary to study the impact of specific surrounding environment. In any cases, the effect of vacuum and temperature variations can be combined with electrons and protons' irradiation, atomic oxygen erosion, and photons impact from UV exposure. On the market, there exist many types of PI, and since several years, composite are also developed. The main properties that are usually observed are the conductivity that is analyzed from surface potential decay, the photoemission and the ability to initiate and propagate surface flashover. Since several years, the space charge storage analysis by the pulse electro-acoustic method has been developed as an interesting complementary tool. It is important to remember that experimental characterization needs to be representative to the space environment especially because it has been observed that PI can recover its original properties in air in a couple of hours depending on the ageing degree.

Keywords: electrostatic discharges, electron and proton irradiation, conductivity, space charge, surface potential decay, secondary emission, photoemission

1. Introduction

Spacecraft evolves in very high-energy radiation environment that is directly dependent on the orbit and sun activity. This harsh environment is composed of high vacuum, energetic electrons and protons' radiations, atomic oxygen, UV exposure, and thermal cycling [1, 2]. A good understanding of the charge accumulation dynamics in dielectrics subjected to the charging space radiative environment is necessary to ensure spacecraft operation reliability [3, 4].

Among the dielectrics that are used in satellites conception, the polyimide (PI) has been selected since quite a long time because it offers excellent electrical and thermal properties [5]. However, the modification of their properties with time under such a specific environment needs to be studied carefully. To do so, large facilities have been developed in laboratories to reproduce the complex spectra that may be encountered in worst configurations [6–8]. Many tests arrangements have been developed and adapted to this specific environment to be able to analyze the properties evolution of materials submitted to various types of external aggression.

The aim of this chapter is to get an overview on experimental results obtained on polyimide (PI) used in space environment. The amount of studies is quite

important and always undergoing so that is why we will focus on main techniques and tendency. Many PIs are available on the market. In order to improve some properties, the production of composite material [9] appears quite interesting as it might allow to reach in a near future a better control on dielectric properties for such specific applications. Qualifications are necessary before sending such a new material in the space environment. This characterization and phase test can take quite a long time.

2. Environment effect on dielectric properties

As already mentioned, when spacecrafts are evolving into space, they are submitted to a large number of charged particles and encounter several operational anomalies. It has been demonstrated that the harmful anomalies are related to spacecraft charging and the risk of electrostatic discharges (ESDs). For instance, Koons et al. [10] established a list of spacecraft accidents between 1973 and 1997, where he shows that 54.2% of the 326 cases analyzed were directly due to ESDs. Other studies confirm the link between ESDs and anomalies recorded on satellites and try to establish links with surface and/or internal charging [11, 12]. The final idea is always to recommend solutions so as to improve satellite's design that mitigate the occurrence of ESD on future spacecraft even if they are submitted to extreme environmental conditions. Many other studies tend to give access to a broad panel of information concerning the origin of those anomalies through the space weather analyses [11, 12].

Usually spacecraft charging is attributed to three main categories called absolute charging, surface charging, and deep-dielectric charging. The absolute charging is associated to the charging of the whole structure versus its environment; the surface charging refers to the external charging and can be associated to the differential charging between the various part of satellites; and at last the deep-dielectric charging concerns the charging in bulk (**Figure 1**). Deep-dielectric charging can occur in materials located on the satellite surface or inside the main structure. It is due to higher energy particles that can cross thick materials on the way without being stopped. In most of the cases, it is surface materials that are studied as they are directly exposed to various sources of ageing and at the origin of most of the discharges.

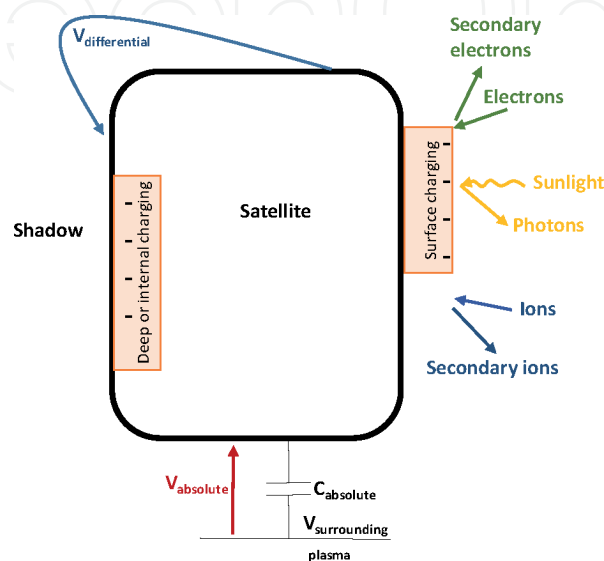


Figure 1.
Schematic representation of satellite charging.

As satellites are made of a large number of materials, it is important to determine surface-material properties and their role in spacecraft surface charging. The main properties that are usually analyzed are:

- the conductivity (surface and bulk)—the accumulation of charges into a dielectric can be responsible for the creation of critic potential difference between adjacent materials from which discharge phenomena can be initiated. In another words, if the conductivity of a dielectric is increased, the differential charging will be limited.
- the dielectric constant as the capability of charge storage will increase if thin samples with high dielectric constant are selected. For instance, 25 μm PI has a dielectric constant close to 3.4.
- the secondary electron emission (SEE) usually dielectric generates more secondary emissions than metals under identical electronic irradiation. Actually the material potential equilibrium will tend toward the second crossover point E_2 (**Figure 2**). This is in favor of a reduction in a dielectric surface potential versus a neighboring metal and might create a disequilibrium at the origin of a discharge.
- the photoemission as the photoelectric effect tends to drive sunlight surfaces more positive than shadowed surfaces and might create differential charging.

2.1 Conductivity and resistivity

The determination of the resistivity of insulating material used in spacecraft conception is very important as it determines how charges will accumulate and will be redistributed during flight. The estimation of an accurate decay time is necessary for the buildup of appropriate spacecraft charging models. As the ohmic resistivity of the PI is too high, the American Society for Testing and Materials (ASTM) method cannot be applied. This is due to the fact of the poor accuracy of pico ampere meter at low current ($<1\text{ pA}$). However, a charge decay resistivity test method was proposed in order to study the ohmic resistivity of high insulation materials [13, 14] and has been adopted by the community. Using this method and fitting surface potential decay (SPD) curves, the ohmic resistivity of PI was estimated to be in the order of $10^{17}\ \Omega\cdot\text{m}$. It occurs to be several order higher than the value estimated by ASTM method.

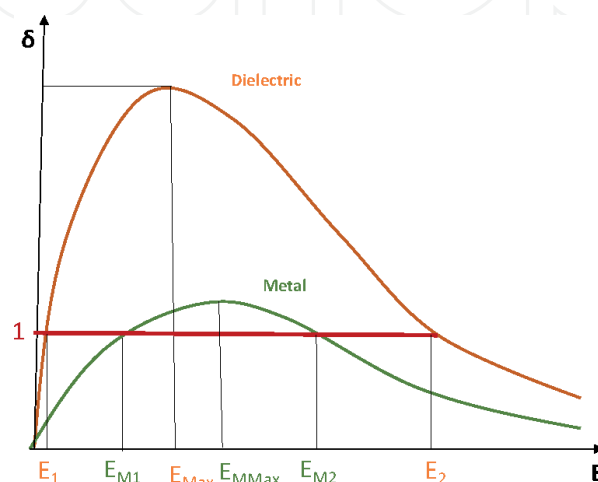


Figure 2.
Secondary emission efficiency for dielectric and metal.

2.1.1 Isothermal surface potential decay experiment

Experimental conditions always need to be carefully controlled. Isothermal SPD is in the range 298–338 k, while the PI sample is irradiated by low-energy electron beam that has been initially recorded. It has been observed that the conductivity is modified as the irradiation goes on and the trapping state gets filled with electrons. That is why depending on the way it is measured, data might be slightly modified.

Besides, we can consider, to some extent that for PI, the photoconduction is a form of radiation-induced conductivity (RIC) as its conductivity can be increased by several decades when exposed to solar lighting with respect to the conductivity in the dark. It has been reported that thin PI films will not charge in sunlight provided that its back surface is grounded. It is therefore recommended to keep PI sample into the dark while SPD is recorded.

The ISPD curve can be separated into three zones: in the part I (transient process), charge trapping and detrapping are competing, whereas in part III (steady state process), the conduction is predominant. In part II, all phenomena are competing [15]. This region limits are difficult to identify that is why most of the time only the initial transient and final steady-state regions are reported on graphs. As surface resistance of spacecraft dielectrics is higher than volume resistances [16], at least one order higher in the case of PI and because external aggression such as atomic oxygen seems to increase the surface resistance without modifying the bulk resistance [17], it is acceptable to neglect the surface charge transport to estimate the bulk conductivity [15]. It is also acceptable to consider that the relative permittivity of PI remains quite stable with the temperature and the electric field during ISPD. However, it was noticed that the surface potential decay is much faster if the initial surface potential is increased. The steady-state current density obtained for a time $t = 3 \times 10^5$ s plotted versus the applied voltage show clearly two regime: ohmic (at low voltage below –950 V) and space charge limited current (at high voltage above –950 V). From the slope, the ohmic resistivity was estimated to $1.2 \times 10^{17} \Omega \cdot \text{m}$ and the effective charge carrier mobility to $1.9 \times 10^{-19} \text{ m}^2/\text{V}\cdot\text{s}$ and the trap density estimated to $1.3 \times 10^{21} \text{ m}^{-3}$. Obviously this type of experiment realized at 298 k needs to be repeated at different temperatures.

Using the 2D ISPD model [18], it is possible to estimate the average surface resistivity, the volume resistivity, and the charge mobility of PI by a genetic algorithm from 298 up to 338 k. In the results reported in **Table 1**, we can observe that the values at 298 k differ a little from the previous estimation by the same authors. This means that these values remain relatively difficult to determine precisely even with the same equipment and the same material. However, the authors managed to calculate the PI surface and volume activation energy and the trap energy which are estimated to 0.3, 0.32, and 0.54 eV, respectively. To get these values, they fitted the surface and volume ohmic resistivity and charge carriers versus the temperature curves using the Arrhenius law.

T (k)	298	308	318	328	338
Surface resistivity ($\times 10^{17} \Omega$)	101.51	42.75	11.66	10.96	3.62
Volume resistivity ($\times 10^{16} \Omega \cdot \text{m}$)	28.70	14.96	4.06	2.14	1.08
Charge mobility ($\times 10^{-19} \text{ m}^2/\text{V}\cdot\text{s}$)	1.49	3.88	6.24	15.60	30.95

Table 1. Surface and volume resistivity estimated from ISPD and simulation with an error of 0.9% [18].

2.1.2 Charge transport model based on deep and shallow traps

In order to model the charge transport in PI, complementary experiment such as thermally stimulated current (TSC) is often performed [19] to investigate the relaxation polarization properties that cannot be easily obtained by dielectric spectroscopy. The charge transport is controlled by high field mechanism as soon as the charging potentials exceed the transition voltage of the ohmic regime. It was reported that the time-dependent permittivity $\epsilon_r(t)$ in PI obeys to Cole-Cole equation rather than Debye ones. Besides, the trap depth could be estimated to be near 1.35 eV [20]. Once released from the surface traps, the charges migrate through the shallow trap to the rear electrode. At 298 k, the carrier residence time was estimated between 7.92×10^{-12} and 1.34×10^4 s in trap depth of 0.1 and 1 eV, respectively [21]. The carriers can easily hop in the shallow traps but will stay in deep traps much longer. Therefore, shallow traps assist conduction processes, whereas deep traps will control the space charge dynamics [22].

It is considered that the shallow traps will control the temperature-dependent hopping at low temperature; then at high temperature, deep traps can also assist the conduction processes as the residence time carriers drops (at 400 k, the residence time carriers in 1 eV trap depth is reduced to 0.648 s). At room temperature, it is reasonable to develop a unipolar charge transport model with a single deep trap level in a first stage (**Figure 3(a)**). It was notice that the surface electrons are easily released from traps surface center whereas they can remain into the bulk for a very long time when they are stored into deep traps. The steady state was reached after 94.8 h; at that time, 39.72% of electrons deposited close to the surface creating a surface potential of -2056 V [21] were released. The resistivity of PI was estimated in the range 8.08×10^{16} – 9.40×10^{16} $\Omega \cdot m$. However, in order to improve the model, it would be better to refine the trap distribution characteristics (**Figure 3(b)**) and consider the density of localized state [23, 24].

2.1.3 Effect of radiation on radiation-induced conductivity

As already mentioned, the RIC is an important phenomenon occurring in PI materials [25]. The RIC can contribute the sample charge decay and prevent discharges. It has been shown that when a step function and uniform irradiation

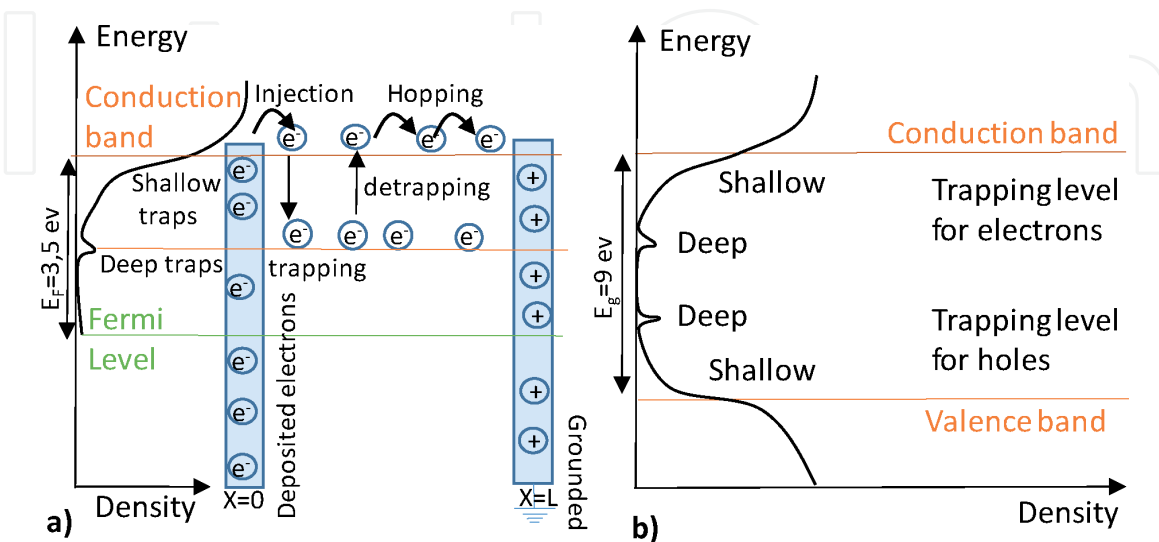


Figure 3. Schematic representation of state density in dielectric materials. (a) Model with one level of deep and shallow traps. (b) Model of shallow and deep traps for electrons and holes that are related to physical and chemical disorder.

are applied, RIC initially rises to a maximum then decreases continuously [26]. In such a case, the accumulation of space charge is not prevented and ESD can be observed.

A different behavior has been observed in various PI (Kapton® 25 µm produced by Dupont© and PM-1-OA 15 µm or PM-1 13 µm produced by Russian services) submitted to large dose rate and long irradiation time [27]. In this study, 40 mm diameter films were Al coated (electrode characteristics: 32 mm diameter and 50 nm thick). They used fresh sample each time even if they mention that an annealing dose effects was observed in PI after 4 h in air at 393 K. For instance, measurements on PM-1 irradiated from 4 up to 10 MeV protons in vacuum (1–4 Pa) and room temperature shows a classic behavior up to a dose of 10⁵ Gy (the dose rate could be in the range 100–5000 Gy/s). Above this dose, the signal increases by two or three orders of magnitude. Even after the end of irradiation, this dose-modified RIC remains much higher than the dark conductivity during a quite a long period of time. An interesting point is that this slow process is completely extinguished as soon as air is introduced into the chamber. The DM RIC effect was attributed to a metastable state in polymers with a strong donor-acceptor interaction that can be easily cancelled by the introduction of atmospheric oxygen. This metastable conjugated structure might be due to the presence of side or inner-chain molecular groups with local conjugation. This strong DM RIC produced by electron of the ambient plasma seems quite useful to reduce the bulk charging of PI used on the outside spacecraft but it is not well controlled. This DM RIC which is a PI intrinsic property prevents the RIC to decay drastically after long irradiation exposure. However, new materials providing, thanks to the introduction of nanoparticles, a better control of the RIC are expected as replacement in the future.

2.1.4 Effect of temperature on conductivity

The effect of temperature has also been studied as spacecraft charging in plasma, and radiative environment is highly sensitive to the temperature decrease which is accompanied by a reduction of the electrical conductivity in dielectric materials [28]. Spacecraft orbiting around the earth are submitted to a large temperature range between 120 and 400 K. It is therefore easy to understand that when dielectric materials are exposed to low temperature, the charge storage increases; whereas when a warming up occurs, a dissipation of this charge can be produced. Experimental setups have been developed in order to study the PI resistivity combining the effect of temperature and electron irradiation to take into account the RIC [29]. First of all, the temperature effect on the volume resistivity was investigated on a Kapton® 200H irradiated for 60 s under a 20 keV electron beam. The useful data reported in **Table 2** have been extracted from the signal recorded for 240 h. The volume resistivity is calculated in the dark region using the expression (Eq. (1)):

$$V(t) = V_0 e^{\left(\frac{-t}{\tau_d}\right)} \quad (1)$$

where $V(t)$ is the surface potential, V_0 is the initial surface potential, and τ_d is the decay time constant in the dark current region. As the temperature increases, the volume resistivity decreases exponentially.

To determine the volume resistivity in short-time region where the polarization current is dominant, Eq. (2) has been used:

$$V(t) = V_o \left[\epsilon_r^\infty + (1 - \epsilon_r^\infty) e^{\left(-\frac{t}{\tau_p}\right)} \right]^{-1} \quad (2)$$

where τ_p is the decay time constant for the decrease in potential due to polarization current; and ϵ_r^∞ corresponds to the relative permittivity when the complete polarization is achieved. The volume resistivity in short time seems to be independent from the temperature, while the volume resistivity in the dark region drops a lot with the increase of the temperature.

Another experiment consists in increasing the energy of the electron beam in addition to the temperature. It shows that when the electrons are injected deeper, the surface potential decay rate increases. This is due to an enhancement of the conductivity produced by trapped electrons in the irradiated area that are responsible for polymer chain scission reaction and the RIC effect. It is particularly true for electrons above 40 keV. It is always important to remember that several effects are combined in real situations that is why the analysis remains quite complex.

2.2 Secondary emission yield

As the electron emission related to irradiated electrons influences the satellite surface charge accumulation, the measurement of the secondary electron emission (SEE) from metal and insulating material used for satellites is quite important. Studies have been performed on material to determine the effect of surface degradation on SEE. The SEE yield is calculated as the ration of the primary incident electron current over the secondary electron current. The shape of the curve represented in **Figure 2** shows E_1 and E_2 , the crossover energy values, where the yield is equal to 1 and the maximum of δ that corresponds to the primary electron energy E_{max} . The SEE Yield (SEY) in solid depends therefore mainly on the primary electron energy E_p , the injection angle, the material density, and the surface status.

2.2.1 Measurement difficulties in polymers

Because of the difficulty in measurement, yield is often neglected as an important contributor into spacecraft charging and therefore the resistivity which is easier to be measured is taken into consideration. Indeed, a full study on the effect

Kapton® 200H 50 µm Temperature (K)	Volume resistivity (Ω.m)	
	Dark current (×10 ¹⁷)	Short time (×10 ¹³)
233	3.3	0.49
253	1.1	1
273	0.83	1.1
299	0.42	1.7
323	0.33	1.3
353	0.11	0.45

Table 2.
Volume resistivity data obtained on Kapton® 200H films irradiated with an 20 keV electron beam for 60 s at different temperatures [29].

of low-fluence electron yield [30] confirms that the electron provided by the measurement system cannot be easily extracted in insulators as in conductor and can affect the measurements. Furthermore, they come to the conclusion that in insulators with modest yield, the incident pulse does not produce enough SE to appreciably charge the specimen under studies. However, in the case of PI with a maximum yield $\sigma_{\max} < 3$ due to the RIC and its persistent effect after the end of the irradiation, charge dissipation is possible and the incident pulse amplitude does not need to be reduced so much. Fortunately, since several years, research is made to improve the measurement system and make it more reliable for polymers and ceramics. The measurement method described in paper [31] shows that very accurate SEEY values can be recorded on Kapton-HN for instance.

2.2.2 Analysis based on frontier molecular orbital theory

Also it was reported that the SEEY of Upilex®-S was smaller than Kapton®-H [32]. This property was explained by a variation in the potential energy bound that can be estimated by quantum chemical calculation which is based on the density function theory. In this representation, the highest occupied molecular orbital (HOMO), corresponding to the conduction band, and the lowest unoccupied molecular orbital (LUMO), corresponding to the valence band, are calculated. For Upilex®-S, the gap between HOMO and LUMO was found to be smaller than for Kapton®-H. The ionization energy that corresponds to the energy difference between the vacuum level and the HOMO was found to be 5.36 eV for Upilex®-S and 5.91 eV for Kapton®-H that comfort the fact that it might be easier to get SEE in the case of Upilex®-S. Such approach needs further investigation.

2.2.3 Effect of atomic oxygen and UV radiations

SEY is really dependent on the surface status of the material under studies. Among all external factors, the atomic oxygen (AO) plays the most important role in the erosion processes of organic materials on the low earth orbit (LEO). It is therefore important to determine the effect of such degradation on PI surface as it might affect quite a lot its SEE properties with time.

To simulate the collision in laboratory, many sources are available [33]. Unfortunately, many AO sources produce VUV radiation during their operation, a fact that should be taken into consideration when comparing results. It was reported that the maximum SEEY of PI film is 1.1 when primary electron energy is 600 eV. Specific work on PI films shows that when the fluence of the AO was increased, the SEE yield was decreased. However, the results were different if the AO was delivered by a laser detonation AO beam source or by the plasma asher method [34]. Usually it is considered that an exposure between 12 and 24 h with a fluence of 3.5×10^{19} and 6.9×10^{19} atom/cm² is respectively equivalent to 6 month and 1 year AO erosion in LEO. The SEE yield was increased in the second case. The difference in the result is due to the source of AO production. It is mentioned that the asher method compared to laser detonation generates AO more easily and avoids contamination which is more representative to what happens in space. The conclusion is that the charging effect of the space plasma should be less effective with time due to AO effect on LEO.

In many cases, the effect of UV and AO are studied simultaneously [35]. In some studies, the total electron emission yield (TEEY) is reported. It corresponds to the sum of the SEEY and the backscatter electron emission yield. The contribution of this phenomenon depends on the electron energy and the material properties [36]. In many cases, the SEEY remains the main source of electron in the TEEY. Similar results are obtained on virgin sample as reported in **Table 3**.

Reference	E_2 (eV)	E_{max} (eV)	σ_{max}	
Virgin—Kapton HN [37] [31]	500	150	1.7	
		180	1.95	
Virgin—Kapton 100 H [35]	670	150	1.69	
UV dose—Kapton 100 H D = 2000 ESH		150	2.1	
			Saturated D > 500 ESH	
AO eroded—Kapton 100 H				
		12 h	500	1.2
		24 h	700	1.0

Table 3. Secondary emission values of cross over energy E_2 , maximum energy E_{max} and yield σ_{max} .

The effect of UV was to increase the TEEY maximum. A saturation was observed above 500 equivalent sun hours (ESH) UV exposure. In PI, UV creates bond scission and provides high concentration of free radicals that are remaining stable for several hours under vacuum as their lifetime is of about 20 h in air. The non-bonded electrons are active and can be excited more easily than bonded electrons that contribute to the increase of the TEEY. However, the UV can penetrate only about 100 nm in materials, whereas energetic electrons (> 3 keV) can go further. The effect of UV is mainly efficient close to the surface where low-energy electrons with a weak penetration depth are supposed to be located.

On addition, the AO erosion acts on both E_{max} and TEEY. The first one increases, whereas the second decreases with the exposure time. The AO acts on the surface roughness. Usually E_{max} and TEEY are expected to increase with the injection angle increase. However, in the case the roughness becomes too important, the secondary electrons might become the source of new primary electrons with lower energies, but the new secondary electrons might not have enough space to escape the surface. That is why as the AO exposure increases, TEEY decreases and E_{max} is significantly increased. The effect of surface roughness was clearly highlighted in the study tempting to demonstrate the effect of surface modification on spacecraft charging parameters [38]. An analysis on Kapton® HN shows that the presence of Dow corning DC 704 diffusion pump oil as surface contaminant oil or scratched produced at the surface during a polishing operation makes the reflectivity to reduce and the absorption coefficient to increase.

2.3 Photoemission yield

When a high frequency light illuminates a dielectric material, the photons interact with the orbital electrons of the atoms. The energy provided to the electrons might be large enough to make them overcome the material work function and become free in vacuum. These electrons are photoelectrons. The photo emission yield (PEY) is the number of photoelectrons to the incident photons. It depends mainly on the incident photon energy, wavelength, and incidence angle but also on the material properties such as absorbance and reflectivity.

It is also important to remember that the photoconduction plays an important role in PI as it is contributing to the RIC. It has been noticed that under constant solar lighting, the conductivity of PI can increase by several decades with respect to conductivity in the dark. Theoretically, PI should not pose any problems of charging under illumination and therefore no electrostatic should be expected. However, it is the surrounding that needs to be considered carefully.

As already mentioned even if spacecraft are operating in the sunlight, some parts will remain in the shadow. The photoemission phenomena maintain the

spacecraft frame and polymers in sunlight to low potential as the photoemission current between the spacecraft and the ambient plasma dominates the current balance equation. On the contrary, polymers in the shadow are charging negatively because the photoemission does not occur and they are mainly impacted by the fast moving electrons of the surrounding plasma.

On the GEO orbit, mainly electron and proton encountered into the Van Allen Belt can lead to the material degradation with time. On LEO, the effects of atomic oxygen and ultraviolet rays are more that need to be considered as harmful as mentioned in the previous section. These UV radiations are responsible for photoemission that might be affected by other degradation with time.

2.3.1 Effect of proton and electron irradiation

Usually the photoemission induced a positive charging at the surface of dielectric that can influence the emission as photoelectron can be attracted back to the surface. That is why during measurements, it is important to choose new area each time by shifting the sample and using short-time exposure to UV pulse. It was shown on Kapton® 100H sample [39] that the proton ageing (in the range 1–15 years equivalent exposure on GEO with 50 keV proton in which penetration depth is estimated by Casino software to be of 600 nm and various flux) makes the PEY to raise. On the contrary, the same ageing with electrons (of 500 keV that can cross the 25 µm sample thickness) seems to make the PEY decay slightly. In both cases, the energy loss by the particles along the way is transmitted to the material, however in the case of proton, this energy is concentrated into the surface shallow layer that might induce high ionization and act in favor of photoemission. In the case of high-energy electron, the energy is deposited in the entire bulk and the surface ionization that might occur is not predominant. It is also important to remember that air exposure can help the sample recovery in a few hours [40]; it is recommended to perform all these measurements while the sample is maintained under vacuum.

2.3.2 Effect atomic oxygen and UV exposure

The UV ageing in the range 25–1000 ESH seems to make the PEY increase but with a saturation above 500 ESH. The same saturation was noticed on secondary electron emission experiments [39]. A study on Kapton®HN, Kapton®E, and Upilex®S showed increases in solar absorptance and the α/ϵ ratio under VUV radiation exposure, whereas emittance changes were not significant [41]. As more photons can be absorbed by damaged PI, the PEY is expected to increase. This effect of absorbance is probably coupled with the chemical degradation and the production of free radical during the UV irradiation [42]. Actually free radicals provide activated electrons that can enhance PEY. At last the AO effect seems to be limited even with the equivalent exposure of 1 year on LEO. In fact, AO increases the surface roughness of the PI film and the photoelectron that are emitted are probably recapture before they can really escape and be detected that is why the PEY tends to decrease with long AO beam exposure.

2.4 Surface flashover

Surface flashover has been identified at triple junction locations on spacecraft [43]. A triple junction is characterized by a metal electrode, a dielectric, and the surrounding environment (air or vacuum). The main theory is based on the secondary electron emission avalanche (SEEA) [44]. The electrons are emitted from the cathode due to field emission. The electrons hit the dielectric surface and

produce secondary electrons. Those electrons continue to move into the direction of the anode under the effect of the electrostatic field. The production of other secondary electrons is made on the way and can be at the origin of an avalanche that produces a degassing and ionization phenomenon on the dielectric surface at the origin of the discharging channel (**Figure 4**).

To understand surface flashover phenomena in space environment, electron irradiation and dc voltage should be considered at the same time. It is also important to take into account the surrounding vacuum [45]. The number of studies combining both effects is growing and has confirmed that the experimental conditions are really sensitive.

The simultaneous action of dc voltage and electron irradiation (**Figure 4**) can be described as follows:

- During electronic irradiation, there is a charge injection and storage in the dielectric bulk. This SC leads to the buildup of an electric field in the bulk that can influence flashover performance.
- During the dc voltage application, a distortion of the electric field at the triple junction (metal/dielectric/vacuum) occurs and electron emission from the cathode is enhanced. The “classic” flashover propagation will occur.

Both phenomena are influencing each other; on one side, the internal electric field (due to the injected charges) creates a reverse-acting force on the kinetic electron flowing to the dielectric surface, and on the other side, the surface electric field might affect the electron injection.

2.4.1 Effect of electron irradiation

It was reported that after electron irradiation, the dc surface flashover of PI was increased due to the electron stored below the surface [46]. Due to the presence of electron in the bulk, the electric field at the triple junction is lowered and then the flashover initiation prevented unless the dc voltage is increased. For instance, the dc voltage flashover on raw polyimide is recorded at 19.2 and 23.9 kV after an irradiation under 20 keV. When the flashover is initiated, the secondary electrons are deviated from the surface and the propagation of the flashover is inhibited. It was noticed that electrons irradiation with an energy above 20 keV up to 30 keV seem to produce the same effect as the penetration depth increases the influence on the surface flashover initiation and propagation might have reached a limit. This tendency was also pointed out on deeply studied PI-type SKPI-MS30 provided by Changzhou

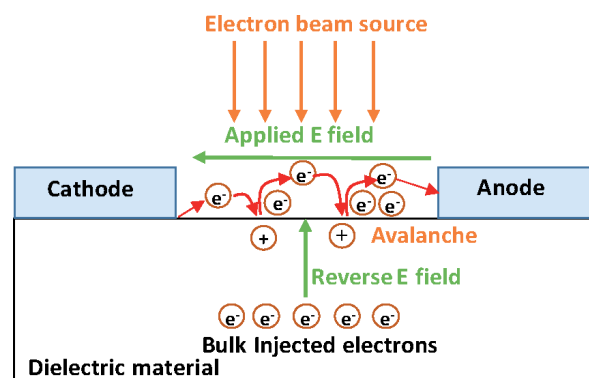


Figure 4.
Surface flashover propagation and combine effect due electron beam irradiation.

Sunchem High Performance Polymer company [47]. It has been observed that above a 20 keV electronic irradiation, the dc surface voltage flashover decreases slightly with the increase of the electron energy. It was also reported in this work that the previously irradiated PI presented higher flashover voltage than the initial sample. They suggest that irradiation could induce chemical-physical modifications such as degradation with the generation of low molecular compounds, gases, and crosslinking. The dielectric constant usually decreases in favor of the diminution of the electric field distortion and deep trap amount increases under low-energy irradiation. These deep traps prevent electrons from migration and favor a charge accumulation that is at the origin of the increase of the dc voltage flashover.

2.4.2 Effect of the electron beam flux

In addition, if the flux of the electron beam is increased (from 0.175 to 1.75 $\mu\text{A}/\text{cm}^2$), the dc surface flashover decreases exponentially with the electron energy. This is explained by the RIC phenomena. During the electron irradiation, electron-holes pairs created can exceed the number of intrinsic carriers and make the RIC to increase. This increase is generally following the energy increase. But when the dose rate increases, the RIC effect decreases and then the effect of accumulated charges increases and contributes to the reduction of the flashover voltage.

2.4.3 Behavior under continuous irradiation

Besides, when measurements are performed during irradiation on the previously irradiated samples, the dc voltage flashover varies. It decreases as the energy of radiation is increased. Starting at 26.9 kV under 5 keV electron irradiation, the dc flashover voltage is of about 10.5 kV under 30 keV electron irradiation. The dc flashover voltage was equal to the value recorded on raw PI under 175 keV electron irradiation. Below this energy, the electrons from the beam are repelled and the dc flashover voltage remains higher than on Virgin PI. On the other hand, when the energy is higher, the electrons can reach the surface and contribute to the flashover phenomenon and the initial dc flashover voltage is decaying. The effect of attraction of the electron of the beam toward the anode is not so important when the energy of the beam is high. The contribution of injected electron below the surface on the electric field distortion is in favor of the reduction of the dc voltage flashover decay.

2.4.4 Influence of vacuum

As mentioned earlier, the effect of vacuum variation is non-negligible. The surface flashover voltage rarely varies in the range of vacuum going from 1.10^{-6} to 6.10^{-1} Pa. However, the decay of the surface flashover voltage is extremely important when the vacuum levels drops. The Paschen's law is controlling the surface voltage flashover above 6.10^{-1} Pa. It could be thought that if the system is maintained in vacuum, as it is the case for satellite environment, these effects could be neglected. However, the pressure can be modified locally above some materials due to a degassing phenomenon. Indeed, it has been shown that the degassing effect can enhance flashover process and should be taken into account in the material selection [48]. Fluorination surface treatment was tested in order to prevent hydrogen degassing from PI samples. The fluorination is realized into a reactor containing a mixed gas composed of 12.5% of fluorine and nitrogen. It was observed that after this surface treatment, the surface flashover voltage was increased by 10.5%. The C–H and C–O bonds are replaced by C–F bonds at the surface which are more stable during the surface flashover and make degas process less effective. Besides, the

electronegativity of the fluorine tends to weaken the avalanche phenomenon and facilitate the electron absorption. This fluorination treatment might be considered as an effective process to reduce flashover due to degassing, but the effect over time should be considered. It might fade with time due to the surrounding aggressions in space.

3. Complementary tools

As discussed in the previous section, there is a large number of conventional tests that have been selected and validated to study material used in a space environment. New tools have been developed to provide complementary information. For instance, the pulse electro acoustic (PEA) method that was commonly used since the 1980s to study the material encountered in electrical engineering application has been adapted to characterize the material under vacuum. This method has been developed to be also efficient to study materials under various conditions such as electron or proton irradiation and under various temperatures in the last 18 years.

3.1 PEA signal recorded after electron irradiation

At first, it was necessary to demonstrate that it is possible to combine measurements of the surface potential and the distribution of charges in the volume by the PEA method. Initial PEA measurements were performed *ex situ* by using a classical system. Then, a specially adapted PEA cell to perform *in situ* measurements during the irradiation was developed [49, 50]. The analysis of surface potential and PEA data provides additional information.

Thanks to the PEA technique, it is possible to follow the buildup of charge into the bulk during an irradiation and then follow the relaxation. The direct observation of the SC distribution with time is providing quite a lot details on the dynamics of the charges migration with time that cannot be obtained by surface potential measurements alone. Depending on their energy, the electrons are expected to be stored at a specific penetration depth that can be predicted by various online programs such as ESTAR [51] that provides, for instance, the range and stopping power in PI. In **Figure 5**, an example of PEA signal recorder on a Kapton®-H film irradiated under a 100 keV electron beam shows a negative peak of injected charges near the back surface in agreement with the theoretical calculation. Thanks to PEA results, it has been shown that the relaxation of these negative charges is quite

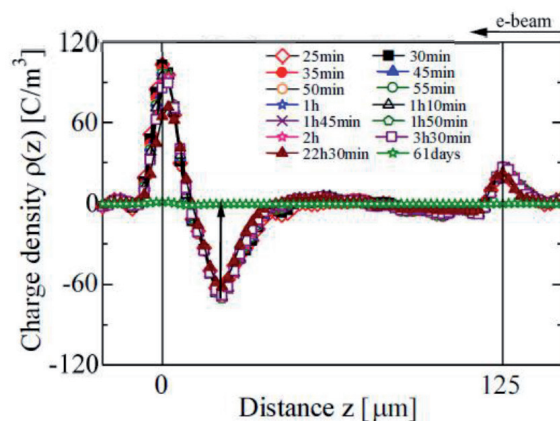


Figure 5. Space charge distribution recorded by PEA on a previously electron irradiated Kapton®-H film. Irradiation conditions: 100 keV with a flux of 1 nA/cm² for 20 min [52].

slow and takes more than 24 h [52] in air. In this case, there was no spreading nor migration of the charge with time as it could be observed in other materials. As mentioned earlier, this type of information cannot be provided by surface potential data.

3.2 Effect of temperature and moisture on space charge distribution

As thermal effect is very important for materials used in space environment, some studies on the impact of temperature on irradiated PI have been realized. At first, a study on the effect of space charge formation under polarization by PEA on Kapton®-H using high electric field (from 110 up to 150 kV/mm) shows that heterocharge accumulates slowly until the breakdown occurs. This effect seems to be accelerated by the temperature when it is increased from 30 to 80°C [53]. Even long short-circuit period could not help to recover initial condition. After an annealing treatment (of at least 150 min in silicon oil at 100°C), it was concluded that the presence of moisture could favor the heterocharge accumulation and breakdown. That is why it is always recommended to take into account the humidity in the atmosphere to characterize PI samples.

X-rays photoelectron spectroscopy (XPS) studies on PI reveals that after a fast thermal cycling (based on IEC-60068-2-14:2009 method), the amount of C–N and C=O bonds increases so as the crystallinity, whereas the amount of C–C and C–O bonds decreases [54]. Due to these modifications, an increase in shallow traps (in the range of activation energy 0.04–0.05 eV) and in the deep traps (in the range of activation energy 0.95–1.31 eV) has been predicted. These alterations are directly linked with the increase of space charge amount detected by PEA during the 60 min polarization under –5 kV. The increase in shallow energy level traps act in favor of charge injection and recombination. In addition, the deep energy level traps make the charges stay into the material after the end of the polarization as observed on the PEA signal.

Another analysis of PEA measurements on a PI irradiated under a 140 keV electron beam at room temperature for various period of time (from 10 to 1800s) then heated up to 135°C has been reported [55]. The buildup of a negative peak into the bulk due to the accumulation of electrons provided by the beam after 10 s of irradiation was clearly observed. An additional negative peak was detected close to the irradiated surface but its origin was not clearly identified. After longer irradiation time, a migration of the negative charges toward the non-irradiated grounded surface was observed. The different patterns of migration accelerated by the temperature are also easy to understand with the representation of the electric field into the bulk. The polarity of the electric field helps to define the direction in which charged particles tend to move. It is also possible to analyze the charge migration into the bulk in combination with thermo-stimulated current (TSC) measurements. A global picture of the charge behavior into the bulk even if only the net charges were observed by PEA can be extracted [56].

3.3 PEA measurements on proton irradiated PI

The PEA technique has been also quite useful to follow the behavior of PI under proton irradiation with different energy on Upilex® S 125 µm films [57]. The energy selected was 1 and 1.5 MeV, and the current density varied from 0.3 to 30 nA/cm² knowing that 0.3 nA/cm² corresponds to the real flux within the inner radiation belts when a solar flare occurs. The irradiation was performed for 10 min. As expected positive charges are detected into the bulk but remain close to the irradiated surface despite the energy as expected by the calculation of proton

range and stopping power by PSTAR [51]. For 1 and 1.5 MeV, the proton penetration depth in PI should be of about 19 and 37 μm , respectively. It was noticed that the SC distribution is highly dependent on the flux. The amplitude of the peak was saturated quickly during irradiation and the relaxation was quite fast for flux higher than 3 nA/cm^2 . This tends to show that some chemical modifications might have happened into the irradiated area. The analysis by XPS UV-vis confirms that molecular scission was produced. Depending on the PI selected, it has been noticed that usually the C–C bond at benzene group increases, whereas C–N bond at imide group and C=O bond at carbonyl of imide group decrease [58]. At last the recovery of the dielectric properties was obtained after a day in air.

4. Conclusions

Polyimide films are used for spatial applications as they offer excellent thermal properties. As they are submitted to various charged particles and radiation during their lifetime, the determination of the ageing effect on such material is really challenging. In laboratories, many irradiation chambers have been developed so as to reproduce and couple the ageing sources such as electron radiation, proton radiation, UV exposure, atomic oxygen surface erosion, and temperature variation. In this chapter, the classic experimental measurements used to study materials for space applications have been presented. It is obvious that the surface potential decay is quite convenient to study the PI conductivity variation under various external conditions. It is also important to be able to characterize the SEE or photoconduction or surface flashover processes in order to mitigate ESD. In addition, the chemical analysis and the use of other techniques such as the PEA method to follow the dynamic of charge buildup and release are important to get a better understanding of the dielectric properties of PI under such an aggressive environment that remains quite difficult to reproduce entirely in laboratories. As mentioned, PI is very sensitive to air exposure, humidity, or UV exposure, so all the experiments must be performed with care in order to provide reliable data for the model that tend to reproduce satellite in its whole structure taking into account the material arrangement so as the surrounding environment.

Author details

Virginie Griseri
LAPLACE, Toulouse University, CNRS, INPT, UPS, Toulouse, France

*Address all correspondence to: virginie.griseri@laplace.univ-tlse.fr

IntechOpen

© 2020 The Author(s). Licensee IntechOpen. This chapter is distributed under the terms of the Creative Commons Attribution License (<http://creativecommons.org/licenses/by/3.0>), which permits unrestricted use, distribution, and reproduction in any medium, provided the original work is properly cited. 

References

- [1] Pisacane VL. *The Space Environment and Its Effect on Space Systems*. 2nd ed. American Institute of Aeronautics and Astronautics: Reston, VA, USA; 2016
- [2] Tribble AC. *The Space Environment*. New Jersey, USA: Princeton University Press; 2003. pp. 1-26
- [3] Baker DN. The occurrence of operational anomalies in spacecraft and their relationship to space weather. *IEEE Transactions on Plasma Science*. 2000;**28**(6):2007-2016. DOI: 10.1109/27.902228
- [4] Gubby R, Evans J. Space environment effects and satellite design. *Journal of Atmospheric and Solar - Terrestrial Physics*. 2002;**64**:1723-1733. DOI: 10.1016/S1364-6826(02)00122-0
- [5] Hastings D, Garrett H. *Spacecraft Environment Interactions*. Cambridge University Press: Cambridge; 1996. pp. 132-177
- [6] Paulmier T, Dirassen B, Belhaj M, Inguibert V, Payan D, Balcon N. Experiment test facilities for representative characterization of space used materials. In: *Proceedings of the 14th ESA/ESTEC SCTC*, Noordwijk, the Netherlands, April 2016. pp. 4-8
- [7] Toyoda K, Masui H, Muranaka T, Cho M, Urabe T, Miura T, et al. ESD ground test of solar array coupons for a greenhouse gases observing satellite in PEO. *IEEE Transactions on Plasma Science*. 2008;**36**(5):2013-2424
- [8] Griseri V, Malaval P, Berquez L, Tung TA, LeRoy S, Boudou L, et al. Charge build-up and transport in electron beam irradiated polymers in a new irradiation chamber. *Annual Report of IEEE International Conference on Electrical Insulation and Dielectric Phenomena*. 2010. DOI: 10.1109/CEIDP.2010.5724030
- [9] Liaw DJ, Wang KL, Huang YC, Lee KR, Lai JY, Ha CS. *Advanced polyimide materials: Syntheses, physical properties and applications*. *Progress in Polymer Science*. 2012;**37**:907-974
- [10] Koons HC, Mazur JE, Selesnick BJF, Fennell JL, Roeder JL, Anderson PC. The impact of space environment on space systems. In: *Proceedings of the 6th Spacecraft Charging Conference*. November 2-6, 1998. MA, USA: AFRL Science Center, Hanscom AFB; 1998. pp. 7-11
- [11] Ferguson DC, Denig WF, Rodriguez JV. Plasma conditions during the galaxy 15 anomaly and the possibility of ESD from subsurface charging. In: *49th AIAA Aerospace Sciences Meeting including the New Horizons Forum and Aerospace Exposition 4-7 January 2011*, Orlando, Florida. 2011
- [12] Iucci N, Levitin AE, Belov AV, Eroshenko EA, Ptitsyna NG, Villosesi G, et al. Space weather conditions and spacecraft anomalies in different orbits. *Space Weather*. 2005;**3**:S01001. DOI: 10.1029/2003SW000056
- [13] Frederickson AR, Dennison JR. Measurement of conductivity and charge storage in insulators related to spacecraft charging. *IEEE Transactions on Nuclear Science*. 2003;**50**(Part 1): 2284-2291
- [14] Dennison JR, Brunson J, Swaminathan P, Green NW, Frederickson AR. Method for high resistivity measurements related to spacecraft charging. *IEEE Transactions on Plasma Science*. 2006;**24**(Part 2): 2191-2203
- [15] Min D, Cho M, Khan AR, Li S. Charge transport properties of dielectrics revealed by isothermal surface potential decay. *IEEE*

Transactions on Dielectrics and Electrical Insulation. 2012;**19**(4):1465-1473

[16] Nitta K, Takahashi M. Material properties measurements related to spacecraft charging/discharging: Current status and future plan. IEEJ Transactions on Fundamentals and Materials. 2009;**129**:739-745. DOI: 10.1541/ieejfms.129.739

[17] Noor DAM, Khan AR, Chiga M, Okumura T, Masui H, Iwata M, et al. Effect of atomic oxygen exposure on surface resistivity change of spacecraft insulator material. Transactions of the Japan Society for Aeronautical and Space Sciences, Aerospace Technology Japan. 2011;**9**:1-8

[18] Min D, Cho M, Khan AR, Li S. Surface and volume charge transport properties of polyimide revealed by surface potential decay with genetic algorithm. IEEE Transactions on Dielectrics and Electrical Insulation. 2012;**19**(2):600-608

[19] Raju GG, Shaikh R, Haq SU. Electrical conduction processes in polyimide films-I. IEEE Transactions on Dielectrics and Electrical Insulation. 2008;**15**(3):663-670. DOI: 10.1109/TDEI.2008.4543102

[20] Tian F, Bu W, Yang C, He L, Wang H, Wang X, et al. A new method for direct determination of trap level distribution from TSC measurement. In: Proceeding of 9th International Conference on Properties and Applications of Dielectric Materials (ICPADM). 2009. DOI: 10.1109/ICPADM.2009.5252276

[21] Min D, Li S, Cho M, Khan AR. Investigation into surface potential decay of polyimide by unipolar charge transport model. IEEE Transactions on Plasma Science. 2013;**41**(12):3349-3358

[22] Teyssedre G, Laurent C. Charge transport modeling in insulating

polymers: From molecular to macroscopic scale. IEEE Transactions on Dielectrics and Electrical Insulation. 2008;**12**(5):857-875

[23] Diahm S, Locatelli ML. Space-charge-limited currents in polyimide films. Applied Physics Letters. 2012;**101**:242905. DOI: 10.1063/1.4771602

[24] Le Roy S, Segur P, Teyssedre G, Laurent C. Description of bipolar charge transport in polyethylene using a fluid model with a constant mobility: Model prediction. Journal of Physics D: Applied Physics. 2004;**37**:298-305. DOI: 10.1088/0022-3727/37/2/020

[25] Plis EA, Engelhart D, Cooper R, Johnston WR, Ferguson D. Review of radiation-induced conductivity effects in polyimide. Applied Sciences. 2019. DOI: 10.3390/app9101999

[26] Tyunev AP, Saenko VS, Poshidaev ED, Ikhsanov RS. Experimental and theoretical studies of radiation-induced conductivity in spacecraft polymers. IEEE Transactions on Plasma Science. 2015;**43**(9):2915-2924

[27] Tyunev AP, Saenko VS, Zhadov A, Poshidaev ED. Radiation-induced conductivity in Kapton-like polymers featuring conductivity rising with an accumulating dose. IEEE Transactions on Plasma Science. 2019;**47**(8):3739-3745

[28] Minow JI, Parker LN. Spacecraft Charging in Low Temperature Environments, 45th AIAA Aerospace Science Meeting. 2007

[29] Watanabe R, Hiroaki H, Okumura T, Takahashi M. Effect of temperature and electron energy on volume resistivity of a polyimide film in space environment. In: IEEE International Conference on Electrical Insulation and Dielectric Phenomena. 2012. DOI: 10.1109/CEIDP.2012.6378870

- [30] Hoffmann R, Dennison JR, Thompson CD, Albretsen J. Low-fluence electron yield of highly insulating materials. *IEEE Transactions on Plasma Science*. 2008;**36**(5):2238-2245
- [31] Hoffmann R, Denisson JR. Measurement method of electron emission over a full range of sample charging. *IEEE Transactions on Plasma Science*. 2012;**40**(2):298-304
- [32] Shibuya K, Nomura K, Miyake H, Tanaka Y, Ochira M, Okumuta T, et al. Development of measurement system for secondary electron emission yield of insulating materials for spacecraft materials. In: *IEEE International Conference on Condition Monitoring and Diagnosis*. 2012. pp. 1102-1105
- [33] Kleiman J, Iskanderova Z, Gudimenko Y, Horodetsky S. Atomic oxygen beam sources: A critical overview. In: *Proceedings of the 9th International Symposium on Materials in a Space Environment, Noordwijk, the Netherlands*. 2003. pp. 313-324
- [34] Nitta K, Miyazaki E, Takahashi M. Influence of atomic oxygen irradiation on secondary electron emission yield of polyimide films. In: *XXIVth International Symposium on Discharges and Electrical Insulation in Vacuum*. 2010
- [35] Wu J, Miyahara A, Khan AR, Iwata M, Toyoda K, Cho M et al. Effect of ultraviolet irradiation and atomic oxygen on total electron emission yield of polyimide. *IEEE Transactions on Plasma Science*. 2014;**42**(1):191-198
- [36] Dennison JR, Sim A, Thomson CD. Evolution of the electron yield curves of insulators as a function of impinging electron fluence and energy. *IEEE Transactions on Plasma Science*. 2006;**34**(5):2204-2218. DOI: 10.1109/TPS.2006.883398
- [37] Balcon N, Payan D, Belhaj M, Tondu T, Inguibert V. Secondary electron emission on space materials: evaluation of the total secondary electron yield from surface potential measurements. *IEEE Transactions on Plasma Science*. 2012;**40**(2):282-290. DOI: 10.1109/TPS.2011.2172636
- [38] Evans A, Dennison JR. The effect of surface modification on spacecraft charging parameters. *IEEE Transactions on Plasma Science*. 2012;**40**(2):305-310
- [39] Wu J, Miyahara A, Khan A, Iwata M, Toyoda K, Cho M, et al. Effects of space environmental exposure on photoemission yield of polyimide. *IEEE Transactions on Dielectrics and Electrical Insulation*. 2015;**22**(2):1204-1212
- [40] Engelhart DP, Plis E, Humagain S, Greenbaum S, Ferguson D, Cooper R, et al. Chemical and electrical dynamics of polyimide film damaged by electron radiation. *IEEE Transactions on Plasma Science*. 2017;**45**(9):2573-2577
- [41] Dever JA, Messer R, Powers C, Townsend J, Wooldridge E. Effects of vacuum ultraviolet radiation on thin polyimide films. *High Performance Polymers*. 2001;**13**:391-399. PII: S0954-0083(01)26273-4
- [42] Peng G, Hao W, Yang D, He S. Degradation of polyimide film under vacuum ultraviolet irradiation. *Journal of Applied Polymer Science*. 2004;**94**:1370-1374
- [43] Cho M. Charging and discharge in vacuum and space. *IEEE International Vacuum Electronics Conference*. 2007. DOI: 10.1109/IVELEC.2007.4283197
- [44] Anderson RA, Brainard JP. Flashover mechanism of pulsed surface flashover involving electron-stimulated desorption. *Journal of Applied Physics*. 1980;**51**:1414. DOI: 10.1063/1.327839
- [45] Pillai AS, Reuben H. Surface flashover of solid insulators in atmospheric air and in vacuum. *Journal*

of Applied Physiology. 1985;58:146.
DOI: 10.1063/1.335700

[46] Li G, Li S, Pan S, Min D. Effect of electron irradiation on dc surface flashover of polyimide in vacuum. *IEEE Transactions on Dielectrics and Electrical Insulation*. 2016;23(3):1846-1853. DOI: 10.1109/TDEI.2016.005429

[47] Liu C, Zheng Y, Yang P, Zheng X, Li Y, Bian E. The DC surface flashover performance research of polyimide under low-energy electron irradiation environment. *IEEE Transactions on Plasma Science*. 2016;44(1):85-92

[48] Wu J, Zhang Z, Ahang B, Ahang L, Zjeng X. Effects of degassing on DC surface flashover property of polyimide. In: *IEEE 11th International Conference on the Properties and Applications of Dielectric Materials (ICPADM)*; 2015

[49] Griseri V, Levy L, Payan P, Maeno T, Fukunaga K, Laurent C. Space charge behaviour in electron irradiated polymers. In: *Annual Report of IEEE International Conference on Electrical Insulation and Dielectric Phenomena*. 2002. pp. 922-925. DOI: 10.1109/CEIDP.2002.1048946

[50] Griseri V, Fukunaga K, Maeno T, Laurent C, Payan D, Levy L. Assessment of measuring conditions with the pulse electro-acoustic system adapted to work under electronic irradiation. In: *Annual Report of IEEE International Conference on Electrical Insulation and Dielectric Phenomena*. 2003. pp. 20-23

[51] ESTAR&PESTAR Program Online. Available from: <https://physics.nist.gov/PhysRefData/Star>

[52] Horiguchi K, Kikuchi Y, Griseri V, Miyake H, Tanaka Y, Berquez L, et al. The relationship between charge decay process and current density differential polyimide and fluoride films irradiated by electrons. In: *International Symposium on Electrical Insulation Materials*. 2014. pp. 381-384

[53] Kishi Y, Miyake H, Tanaka Y, Takada T. Relationship between breakdown and space charge formation in polyimide film under dc high stress. In: *Annual Report of IEEE International Conference on Electrical Insulation and Dielectric Phenomena*. 2009. pp. 146-149

[54] Qin S, Tu Y, Wang S, Cheng Y, Chen B, Wang C, et al. Accelerated aging of fast thermal cycle effects on the behavior of space charge in polyimide. *IEEE Transactions on Dielectrics and Electrical Insulation*. 2017;24(52017):3182-3190. DOI: 10.1109/TDEI.2017.006483

[55] Sato S, Yanagisawa S, Tanaka Y, Watanabe R, Tomita N. Investigation of space charge behavior in polyimide film during elevating temperature. In: *Annual Report of IEEE International Conference on Electrical Insulation and Dielectric Phenomena*. 2007. pp. 57-60

[56] Takada T, Kitajima H, Kodaka M, Tanaka Y. Analysis of conduction current in electron-beam irradiated PMMA by simultaneous measurement of thermally stimulated current and space charge distribution. In: *Annual Report of IEEE International Conference on Electrical Insulation and Dielectric Phenomena*. 1997. pp. 463-466

[57] Numat S, Miyake H, Tanaka Y, Takada T. Dielectric characteristic evaluation of proton beam irradiated polyimide films. In: *Annual Report of IEEE International Conference on Electrical Insulation and Dielectric Phenomena*. 2010

[58] Miyake H, Uchiyama R, Tanaka Y. The relationship between charge accumulation and scission of molecular chain in the proton irradiated PI. In: *IEEE International Conference on Solid Dielectrics*. 2016. DOI: 10.1109/ICD.2016.7547562